RESEARCH ARTICLE

Editorial Process: Submission:01/18/2024 Acceptance:06/11/2024

Improving the Feasibility of Mitigating Phase Errors in 4DCT caused by a Random Reference Breathing Pattern in the Quasar Phantom and the Role of Slice Thickness

Arun Balakrishnan[1,2], Padmanabhan Ramesh Babu[2]*

Abstract

Purpose: The study aimed to validate a method for minimizing phase errors by combining full-length lung 4DCT (f4DCT) scans with shorter tumor-restricted 4DCT (s4DCT) scans. It assessed the feasibility of integrating two scans one covering the entire phantom length and the other focused on the tumor area. The study also evaluated the impact of Maximum Intensity Projection (MIP) volume and imaging dose for different slice thicknesses (2.5mm and 1.25mm) in both full-length and short target-restricted 4DCT scans. **Methods:** The study utilized the Quasar Programmable Respiratory Motion Phantom, simulating tumor motion with a variable lung insert. The setup included a tumor replica and a six-dot IR reflector marker on the breathing platform. The objective was to analyze volume differences in fMIP_2.5mm compared to sMIP_1.25mm within their respective 4D_MIP CT series. This involved varying breathing periods (2.5s, 3.0s, 4.0s, and 5.0s) and longitudinal tumor sizes (6mm, 8mm, and 10mm). The study also assessed exposure time and expected CTDIvol of s4D_2.5mm and s4D_1.25mm for different breathing periods (5.0s to 2.0s) in the sinusoidal wave motion of the six-dot marker on the breathing platform. **Results:** Conducting two consecutive 4DCT scans is viable for patients with challenging breathing patterns or when the initial lung tumor scan is in close proximity to the tumor location, eliminating the need for an additional full-length 4DCT. The analysis involves assessing MIP volume, imaging dose (CTDIvol), and exposure time. Longitudinal tumor shifts for 6mm are [16.6-17.2] in fMIP_2.5mm and [16.8-17.5] in sMIP_1.25mm, for 8mm [17.2-18.3] in fMIP_2.5mm and [17.8-18.4] in sMIP_1.25mm, and for 10mm [19-19.9] in fMIP_2.5mm and [19.4-20] in sMIP_1.25mm ($p \geq 0.005$), respectively. **Conclusion:** The Quasar Programmable Respiratory Motion Phantom accurately replicated varied breathing patterns and tumor motions. Comprehensive analysis was facilitated through detailed manual segmentation of Internal Target Volumes and Internal Gross Target Volumes.

Keywords: Tumor-restricted- s4DCT- tumor localization- treatment planning- respiratory motion

Asian Pac J Cancer Prev, **25 (6)**, 2089-2098

Introduction

In the context of binning 4DCT (4-Dimensional Computed Tomography) scans for lung patients, the occurrence of phase errors represents a persistent challenge. These errors, varying from minor discrepancies to significant inaccuracies, can compromise treatment planning quality and influence patient outcomes [1-5]. A primary contributor to these phase errors is the difficulty in consistently adhering to reference breathing patterns, especially when scans encompass the entire length of the lungs and liver. Patients, particularly those undergoing radiation therapy or diagnostic imaging, often need to control their breath or maintain a consistent breathing pattern during scans to obtain precise images capturing the dynamic motion of tumors and surrounding tissues [6-9]. However, adherence to these patterns becomes more challenging when the scan covers a larger anatomical region, such as the entire lungs and liver.

In the context of Axial 4DCT within the Real-Time Position Management (RPM) System by Varian, the quest for precision and the reduction of phase errors hinges on maintaining the patient's consistency in their repeated breathing patterns and intervals. This approach is grounded in foundational assumptions in 4DCT, assuming regular patient breathing patterns, a consistent temporal relationship between external surrogates and internal target motion, and sufficient data for image reconstruction at all specified breathing states [10-17]. However, practical clinical scenarios often disrupt these assumptions due to irregular breathing patterns, resulting in image artifacts. Lung 4DCT scans frequently exhibit such artifacts, stemming from irregular breathing and suboptimal scan parameters. Factors contributing to these artifacts include

*[1]Division of Medical Physics, Department of Radiation Oncology, Tata Medical Center, Newtown, Rajarhat, Kolkata, West Bengal, India. [2]Department of Physics, School of Advanced Sciences, Vellore Institute of Technology, Vellore, Tamil Nadu, India. *For Correspondence: prameshbabu@vit.ac.in*

variations in breathing pattern amplitudes and frequencies, instances of coughing, temporary breath-holding due to patient fatigue during extended repetitions, prolonged scan durations, and shifts in the baseline of the breathing pattern [18-23]. Consequently, addressing these issues requires adjustments in scan parameters, particularly concerning image acquisition times determined by the CT scanner based on the patient's breathing periods as provided by the Real-Time Position Management (RPM) system from Varian.

Despite thorough training sessions and recommendations from entities such as the SABR UK Consortium, a significant number of lung 4DCT scans still struggle to maintain the expected repeated breathing wave patterns and intervals among patients. This highlights a fundamental challenge in achieving the idealized conditions for 4DCT scans [24-31]. Two pivotal factors further exacerbate the situation: the scan duration for 2.5 mm slice thickness and the dosage of imaging. The duration of 4DCT imaging scans is closely tied to the duration of a patient's breathing cycle and the complete scan length. Patient breathing cycles typically vary between 2.2 seconds and 4.5 seconds, and any prolongation in this cycle directly extends the scan duration. These scans typically cover the entire lung and liver to assess dose-related metrics such as V20 for lungs and the mean liver dose, all within established tolerance levels for treatment planning [37]. However, an elongated imaging scan time can increase the likelihood of encountering phase errors in the 4DCT scans. These errors manifest as image slices that are not synchronized in time with their preceding or successive counterparts. This asynchrony can occur at various points within the tumor's motion cycle, affecting the reconstruction of the tumor's features in Maximum Intensity Projection (MIP), Average Intensity Projection (Avg-IP), and Minimum Intensity Projection (Min-IP) CT image sets [33-40]. The resultant phase errors introduce uncertainty in estimating the projection of the tumor, thereby complicating the determination of the Internal Target Volume (ITV). Using a tumor-restricted length of short 4DCT (s4DCT) scans in conjunction with standard full-length lung 4DCT (f4DCT) scans, this phantom study sought to evaluate a workflow for minimizing phase errors.

In this technique, the aim is to evaluate the practicability of binning DICOM-tagged two 4DCT scans by combining a standard 4DCT scan of the entire 15cm phantom with an extended scan focusing on the target-restricted length. Subsequently, the study involves a comparative analysis and quantification of volume disparities between Maximum Intensity Projection (MIP) images derived from 2.5mm slice thickness full 4DCT (f4D_2.5) and MIP images from 2.5mm and 1.25mm slice thickness short target-restricted length 4DCT scans (s4D_2.5 and s4D_1.25). The investigation specifically concentrates on the Hounsfield Unit (HU) range of -350 to 1050, employing a designated window selection to minimize inter-observer variation. Furthermore, the research aims to examine how volume differences fluctuate with distinct breathing periods (2.5 sec, 3.0 sec, 4.0 sec, and 5.0 sec). Additionally, the study delves into the impact of varying longitudinal tumor sizes (6mm, 8mm, and 10mm) on the observed volume differences.

Materials and Methods

This proposed study aims to explore the potential advantages of improving the precision and accuracy of tumor localization in 4DCT scans, with a particular emphasis on the influence of different slice thicknesses. The rationale behind this investigation stems from the acknowledgment that phase errors can significantly impact the dependability of these scans, potentially compromising the quality of patient care [32]. In instances where 2.5 mm slice 4DCT scans exhibit an elevated occurrence of phase errors or encounter challenges in reproducing the reference breathing pattern consistently, a novel approach is suggested. This strategy involves enhancing the workflow by incorporating a 1.25 mm slice 4DCT imaging procedure specifically targeting the region of interest (ROI) containing the tumor. A supplementary margin of 3-5 cm is added from both the superior and inferior ends of the tumor to ensure comprehensive coverage.

The complete sequence of the 4DCT scan, specifically employing a finer slice thickness of 1.25 mm (referred to as f4D_2.5) depicts in Figure 1. The primary rationale for adopting this finer slice thickness is to elevate image resolution. This enhancement in resolution facilitates a more precise delineation of the Internal Target Volume (ITV) of the tumor in comparison to the conventional 2.5 mm slice thickness. Consequently, the imaging data acquired with the 1.25 mm slice width offers richer information regarding the tumor's boundaries and motion dynamics. One of the significant advantages of this proposed method is a substantial reduction in imaging time. The 1.25 mm slice thickness 4DCT imaging process consumes approximately one-third of the time required for a full 4DCT scan utilizing a 2.5 mm slice thickness. This time-saving characteristic not only improves patient comfort but also diminishes the likelihood of motion artifacts that may arise from prolonged scan durations.

Two distinct 4DCT scans: one with a slice thickness of f4D_2.5 and another presenting proposed options s4D_2.5 or s4D_1.25 illustrates in Figure 2. To verify the feasibility and efficacy of this proposed approach, a thorough phantom study was conducted. This study utilized the Quasar Programmable Respiratory Motion

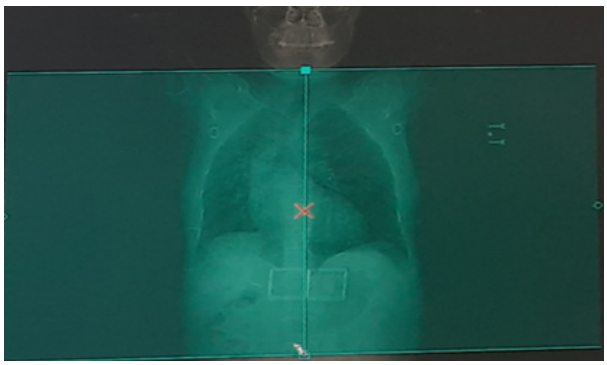

Figure 1. Routine Full Length of the 4DCT (f4D_2.5)

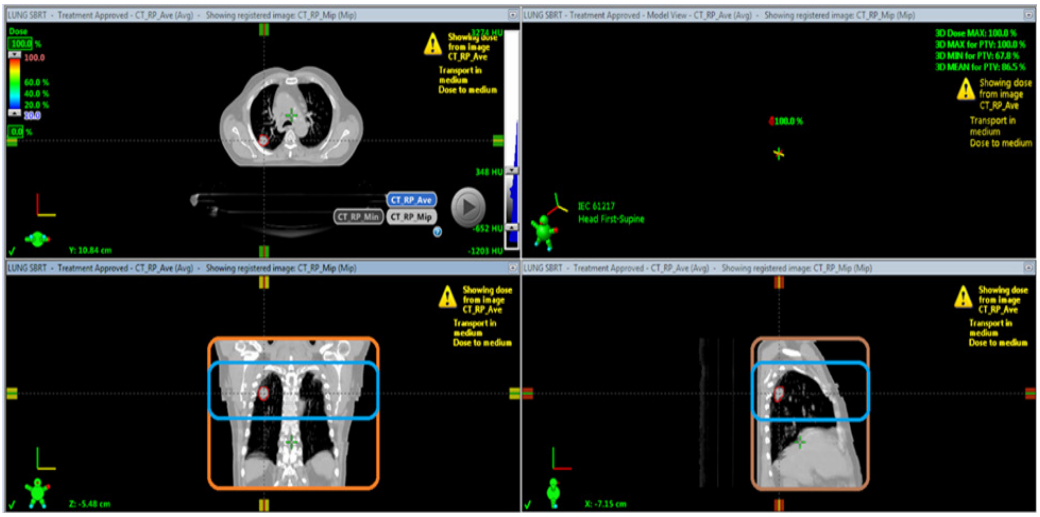

Figure 2. 4DCT Scan Length of f4D_2.5 and Proposed s4D_2.5 or s4D_1.25 Depicted as Orange and Cyan Colour

Phantom, an advanced tool crafted to replicate lung tissue and tumor motion accurately. The phantom simulated sinusoidal motion breathing patterns closely resembling real patient conditions, encompassing variations in both breathing period and tumor displacement [20]. The tracking of breathing patterns and tumor motions was executed using the Varian RPM system, which employs infrared camera technology to monitor a six-dot marker on the phantom's breathing platform. Subsequently, this data guided the acquisition of 4DCT scans on a GE Wipro Light Speed Xtra 16-slice CT scanner. The resulting 4DCT images, obtained with both 2.5 mm and 1.25 mm slice thicknesses, underwent processing to generate Maximum Intensity Projection (MIP) and Average Intensity Projection (Avg-IP) images. The Internal Target Volume (ITV) and Internal Gross Tumor Volume (iGTV) were meticulously segmented and analyzed using Hounsfield Units (HU) window selection to ensure consistency and reproducibility in data interpretation.

Methodology Validation

Methodology validation through a phantom study represents a pivotal phase in the development and refinement of advanced medical imaging techniques, such as tumor-restricted s4DCT (4-Dimensional Computed Tomography) [26]. This controlled experimental setting serves as a crucial intermediate step before implementing novel methodologies in real clinical scenarios. In the context of tumor-restricted 4DCT, the primary objective of a phantom study is to evaluate and confirm the method's efficacy in minimizing phase errors. Phantom studies utilize synthetic models that replicate the anatomical and physiological characteristics of actual patients [11]. Constructed with materials mimicking human tissues, these models create a highly controlled experimental environment, allowing precise manipulation of variables and observation of outcomes.

In the case of tumor-restricted 4DCT, phantoms enable researchers to simulate scenarios where tumors within the body exhibit intricate motion patterns, often influenced by respiration [7]. By introducing controlled motion into these phantoms, researchers can closely replicate the dynamic conditions encountered in real patients. Through such experimentation, researchers can thoroughly assess how tumor-restricted 4DCT affects the reduction of phase errors. They can compare the outcomes of this technique with those obtained using traditional 4DCT methods, examining the extent to which the novel approach mitigates phase errors.

A primary advantage of conducting a phantom study is its ability to provide both quantitative and qualitative data [41]. Researchers can measure the accuracy, precision, and reliability of tumor-restricted 4DCT in reducing phase errors, offering tangible evidence of the method's potential effectiveness. Additionally, the use of phantoms allows researchers to iterate and refine the methodology, addressing any unforeseen challenges or limitations. This approach serves as a safety net, enabling scientists and clinicians to troubleshoot and optimize the technique before applying it to actual patients.

Quantifying Phase Error Reduction

The reduction of phase errors is a critical component of evaluating the effectiveness of innovative techniques such as tumor-restricted s4DCT (4-Dimensional Computed Tomography). Phantom studies serve as an ideal platform for precisely quantifying the degree of phase error reduction, a crucial step in ensuring the reliability and clinical applicability of these advanced methods [39]. In the course of a phantom study, researchers establish a controlled experimental environment that closely mimics real patient conditions. Within this framework, they can systematically manipulate and quantify variables to gauge the impact of tumor-restricted 4DCT on phase errors. To initiate the quantification process, researchers employ synthetic phantoms designed to replicate the physiological and anatomical features of human bodies. These phantoms are capable of simulating dynamic motion patterns exhibited by tumors, often influenced by respiration [5]. Through these phantoms, researchers can induce controlled motion that closely emulates the complexities of real patient scenarios.

By comparing the results obtained from tumor-restricted 4DCT with those derived from standard 4DCT techniques, researchers can quantitatively assess the degree of phase error reduction. This direct comparison furnishes concrete evidence of the efficacy of the novel approach. Quantification entails measuring specific metrics related to phase errors [23]. Researchers can evaluate the accuracy and precision of tumor localization, directly quantifying how the innovative methodology enhances this process. Furthermore, they can assess the potential impact of phase error reduction on treatment planning, particularly in the context of radiation therapy. This quantification extends to both spatial and temporal dimensions, ensuring a comprehensive evaluation of the technique's performance.

Clinical Translation Potential

The clinical translation potential of innovative medical imaging techniques, such as tumor-restricted s4DCT (4-Dimensional Computed Tomography), is a crucial step in bridging the gap between research and patient care. Phantom studies, which provide controlled environments for validation, play a pivotal role in assessing the feasibility and benefits of such methods [12]. If a phantom study reveals significant phase error reduction, it can open the door to the clinical implementation of tumor-restricted s4DCT, with profound implications for the field of medical imaging and cancer treatment. The promise of reduced phase errors in the clinical setting is particularly significant for radiation therapy, a cornerstone of cancer treatment. Accurate tumor localization and precise treatment planning are essential for optimizing the effectiveness of radiation therapy [2]. Phase errors, which can affect the accuracy of target delineation, have a direct impact on the radiation dose delivered to the tumor and surrounding healthy tissue. Reducing phase errors through tumor-restricted s4DCT can lead to more precise radiation therapy, increasing the likelihood of tumor control while minimizing damage to nearby structures.

In addition to enhancing the precision of radiation therapy, the clinical implementation of tumor-restricted s4DCT can have broader implications for cancer patients. It may lead to better treatment outcomes, improved quality of life, and reduced side effects [25]. Reducing the uncertainty associated with tumor motion and the corresponding treatment planning adjustments, this approach can minimize unnecessary radiation exposure to healthy tissues, thereby reducing the risk of collateral damage and side effects [34]. Furthermore, the potential for clinical translation does not stop at radiation therapy. Tumor-restricted s4DCT can also benefit other medical interventions, such as surgical planning and guidance. Improved accuracy in localizing tumors can enhance surgical procedures by providing surgeons with more precise information about tumor position and motion.

Results

Examining a longitudinal tumor shift of 6mm (±3mm), the study investigates the influence of different breathing periods on volumes of interest. Across various breathing periods (2.5, 3.0, 4.0, and 5.0 seconds), minimal variations are observed in the recorded volumes for fMIP_2.5mm, sMIP_2.5mm, and sMIP_1.25mm, all measured in cubic centimeters (CC). The volumes show consistent values, indicating stability across the range of breathing periods. To assess potential significant differences in breathing patterns and times among fMIP_2.5mm, sMIP_2.5mm, and sMIP_1.25mm for tumor sizes of 6mm, 8mm, and 10mm, a one-way ANOVA test was employed. Table 1 presents the identified breathing parameters along with the specific time span for a 6mm tumor.

The statistical analysis, represented by the P-values, and Confidence Interval using one-way Anova test, reveals that these differences are not statistically significant (NS), indicating that the observed changes in volume are likely due to random variations rather than the specific breathing period. Similarly, for an 8mm (±4mm longitudinal tumor shift), the trend continues (Table 2).

Table 3 displays the respiratory parameters and duration of fMIP_2.5mm and sMIP_2.5mm for a 10mm scenario. Across varying breathing periods from 2.5 seconds to 5.0 seconds, minimal fluctuations are observed in the volumes of fMIP_2.5mm, sMIP_2.5mm, and sMIP_1.25mm. Statistical analysis, with P-values labeled as NS (non-significant), consistently indicates that these volume disparities lack statistical significance.

Also, Table 3 depicts the shifting ratio with time and P value in the longitudinal shift. For a breathing period of 2.5 seconds, the recorded volumes (in CC, cubic centimeters) for fMIP_2.5mm and sMIP_2.5mm are consistently 19.0 CC, while sMIP_1.25mm exhibits a slightly larger volume of 19.4 CC. The P-value of 0.777 (NS) indicates that these volume differences are not statistically significant. A similar trend is observed across different breathing periods (3.0, 4.0, and 5.0 seconds), where the volumes for fMIP_2.5mm, sMIP_2.5mm, and sMIP_1.25mm show minimal variations. The P-values for each comparison remain greater than 0.05, denoted as NS, confirming that the observed volume differences are not statistically significant.

Table 4 highlights the extended longitudinal

Table 1. Breathing Parameters and Time of fMIP_2.5mm, sMIP_2.5mm and sMIP_1.25mm for 6mm (±3mm Longitudinal Tumor Shift)

Breathing Period (Sec)	fMIP_2.5mm Volume (CC)	sMIP_2.5mm Volume (CC)	sMIP_1.25mm Volume (CC)	SD	P value	Confidence Interval
2.5	16.6	16.6	16.8	0.115	0.787, NS	0.130664
3	16.9	16.9	17	0.057	0.856, NS	0.065292
4	17.1	17.1	17.3	0.115	0.976, NS	0.130664
5	17.2	17.2	17.5	0.173	0.921, NS	0.195991

Table 2. Breathing parameters and Time of fMIP_2.5mm sMIP_2.5mm and sMIP_1.25mm for 8mm (±4mm longitudinal tumor shift)

Breathing Period (Sec)	fMIP_2.5mm Volume (CC)	sMIP_2.5mm Volume (CC)	sMIP_1.25mm Volume (CC)	SD	P value	Confidence Interval
2.5	17.2	17.2	17.8	0.34641	0.876, NS	0.391981
3	17.7	17.7	18	0.1732	0.898, NS	0.195991
4	18	18	18.3	0.1732	0.987, NS	0.195991
5	18.3	18.3	18.4	0.05773	0.884, NS	0.065292

displacement at 6mm, 8mm, and 10mm. Specifically focusing on a 6mm (±3mm longitudinal tumor shift), the data contrasts volumes (in CC, cubic centimeters) between fMIP_2.5mm and sMIP_1.25mm across various breathing periods. The "Difference" column quantifies the volume change magnitude between these measurements, with denoting their intersection and representing their union. The Jaccard Index (JI), expressing the intersection over the union as a percentage, gauges the similarity between A and B, with a higher JI indicating greater similarity. The Dice Similarity Index (DSI) evaluates the overlap between A and B, with a higher DSI signifying more substantial overlap. The Geometric Mean Increase (GMI) denotes the percentage volume increase for B relative to A. Additionally; the Dice Index (DI) assesses the similarity between A and B, with a lower DI indicating greater similarity.

For 6mm of fMIP_2.5mm and sMIP_1.25mm, the longitudinal tumor shift is [16.6-17.2] and [16.8-17.5], for 8mm of fMIP_2.5mm it is [17.2-18.3] and sMIP_1.25mm [17.8-18.4], and for 10mm of fMIP_2.5mm it is [19-19.9] and sMIP_1.25mm [19.4-20] ($p \geq 0.005$), respectively. The breathing period spans 2.5–5 seconds. The JI values for sMIP_1.25mm and fMIP_2.5mm are computed for a 6mm longitudinal tumor shift (±3 mm), yielding a result of 97.6190476–98.265896. From 0.98203593 to 0.97982709, the DSI value falls. The JI values for fMIP_2.5mm and sMIP_1.25mm are calculated for 8mm (±4mm longitudinal tumor shift), which increases from 97.1428571 to 98.3695652, with a breathing period ranging from 2.5 to 5 seconds. Additionally, the DSI value rises from 0.97142857 to 0.98637602. Finally, the JI values for fMIP_2.5mm and sMIP_1.25mm are calculated as 95.8762887 to 97.5 for 10mm (±5mm longitudinal tumor shift). Additionally, the DSI value rises from the 0.96875–0.997744361 range. The longitudinal tumor shift for 6mm, 8mm, and 10mm does not exhibit an error, according to the GMI values.

Across different breathing periods, it is evident that the differences in volume between fMIP_2.5mm and sMIP_1.25mm are generally minimal. The JI, DSI, and DI values remain close to one, suggesting a high level of similarity. The GMI values are also relatively low, indicating a minimal volume increase in sMIP_1.25mm. These findings emphasize the consistency of volume measurements between the two imaging techniques.

The relationship between slice thickness (in mm), breathing period (in seconds), and CTDI vol (mGy) for both s4D_2.5 and s4D_1.25 scans displays in Figure 3. For the 2.5 mm slice thickness, as the breathing period decreases, there's a corresponding reduction in CTDI vol, reflecting shorter exposure times. The values remain consistent between s4D_2.5 and s4D_1.25 scans at 133.81 mGy for 5.0 seconds, 122.15 mGy for 4.5 seconds, and so forth, down to 67.02 mGy for 2.0 seconds. The latter part of the table, pertaining to 1.25 mm slice thickness, is incomplete, and data for CTDI vol is missing. However, it is expected that similar trends of decreasing CTDI vol

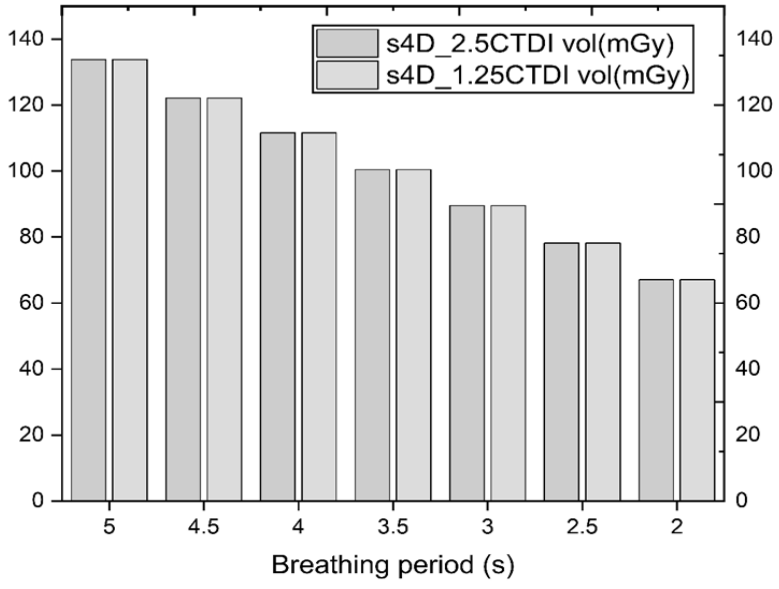

Figure 3. s4D_1.25CTDI vol (mGy) vs s4D_2.5CTDI vol (mGy)

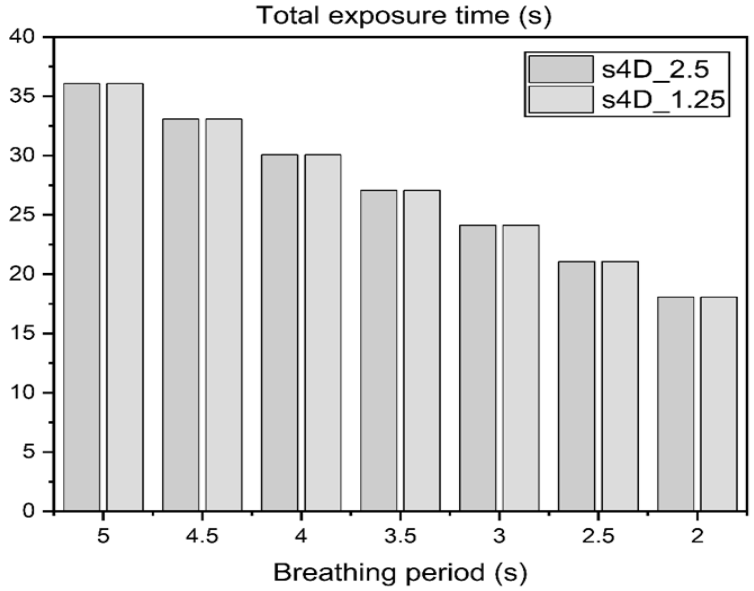

Figure 4. s4D_2.5 vs s4D_1.25 Total Exposure Time

with shorter breathing periods would continue.

The relationship between breathing periods (in seconds) and the total exposure time (in seconds) for both s4D_2.5 and s4D_1.25 scans represent in Figure 4. As the breathing period decreases, there is a corresponding reduction in the total exposure time for both imaging techniques. Regardless of the specific breathing period, the total exposure time remains consistent at 36.06 seconds for 5.0 seconds, 33.06 seconds for 4.5 seconds, and so forth, down to 18.06 seconds for a breathing period of 2.0 seconds. This data highlights the predictable and constant total exposure times for different breathing periods, emphasizing the relationship between scan parameters and radiation exposure in these scans.

The number of images acquired in both s4D_2.5 and s4D_1.25 scans indicates in Figure 5. Remarkably, the number of images remains consistent across all breathing periods, with 264 images in s4D_2.5 and 528 images in s4D_1.25 scans. This consistency in image acquisition suggests that the scan parameters are well-defined and do not vary with different breathing patterns. The reliability in the number of acquired images across various breathing periods ensures consistency in the quality of data and imaging, which is critical for accurate clinical evaluations and radiation therapy planning.

Discussion

This comprehensive study aimed to evaluate the applicability of three distinct clinical imaging modalities (Full 2.5, Short 2.5, Short 1.25) for radiotherapy management in lung cancer patients with irregular

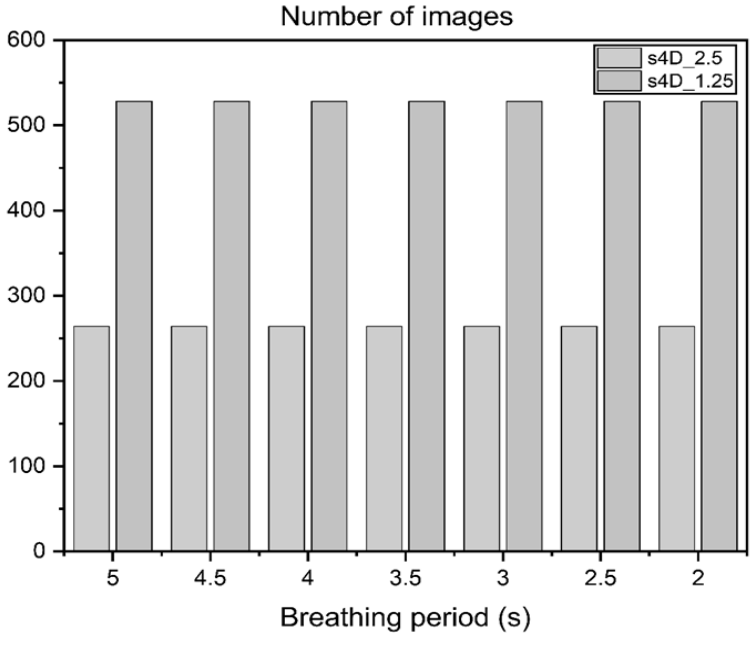

Figure 5. Comparison of Number of Slice Images of s4D_2.5 and s4D_1.25

Table 3. Breathing Parameters and time of fMIP_2.5mm sMIP_2.5mm and sMIP_1.25mm for 10mm (±5mm longitudinal Tumor Shift)

Breathing Period (Sec)	fMIP_2.5mm Volume (CC)	sMIP_2.5mm Volume (CC)	sMIP_1.25mm Volume (CC)	SD	P value	Confidence Interval
2.5	19	19	19.4	0.23094	0.777, NS	0.261328
3	19.2	19.2	19.5	0.173205	0.854, NS	0.195991
4	19.6	19.6	19.8	0.11547	0.888, NS	0.130664
5	19.9	19.9	20.1	0.11547	0.965, NS	0.130664

Table 4. Longitudinal Shift

6mm (±3mm longitudinal tumor shift)									
Breathing Period (Sec)	fMIP_2.5mm Volume (CC)	sMIP_1.25mm Volume (CC)	Difference	A ∩ B	A U B	JI=(|A ∩ B|/|A U B|)*100	DSI=2* (A ∩ B)/(A + B)	GMI= B-(A ∩ B)/B	DI = 1 - ((A ∩ B)/A)
2.5	16.6	16.8	0.2	16.4	16.8	97.6190476	0.98203593	0.02380952	0.01204819
3	16.9	17	0.1	16.8	17	98.8235294	0.99115044	0.01176471	0.00591716
4	17.1	17.3	0.2	16.9	17.2	98.255814	0.98255814	0.02312139	0.01169591
5	17.2	17.5	0.3	17	17.3	98.265896	0.97982709	0.02857143	0.01162791
8mm (±4mm longitudinal tumor shift)									
Breathing Period (Sec)	fMIP_2.5mm Volume (CC)	sMIP_1.25mm Volume (CC)	Difference	A ∩ B	A U B	JI=(|A ∩ B|/|A U B|)*100	DSI=2* (A ∩ B)/(A + B)	GMI= B-(A ∩ B)/B	DI = 1 - ((A ∩ B)/A)
2.5	17.2	17.8	0.6	17	17.5	97.1428571	0.97142857	0.04494382	0.01162791
3	18.1	18	0.3	17.5	18	97.2222222	0.96952909	0.02777778	0.03314917
4	18	18.3	0.3	17.8	18.1	98.3425414	0.98071625	0.0273224	0.01111111
5	18.3	18.4	0.1	18.1	18.4	98.3695652	0.98637602	0.01630435	0.01092896
10mm (±5mm longitudinal tumor shift)									
Breathing Period (Sec)	fMIP_2.5mm Volume (CC)	sMIP_1.25mm Volume (CC)	Difference	A ∩ B	A U B	JI=(|A ∩ B|/|A U B|)*100	DSI=2*(A ∩ B)/(A + B)	GMI= B-(A ∩ B)/B	DI = 1 -((A ∩ B)/A)
2.5	19	19.4	0.4	18.6	19.4	95.8762887	0.96875	0.04123711	0.02105263
3	19.2	19.5	0.3	18.9	19.4	97.4226804	0.97674419	0.03076923	0.015625
4	19.6	19.8	0.2	19.3	19.6	98.4693878	0.97969543	0.02525253	0.01530612
5	19.9	20	0.1	19.5	20	97.5	0.97744361	0.025	0.0201005

DSI (Dice Similarity coefficient) Tol: Value 1= perfect overlap; 0= No overlap; >0.7 = poor agreement; GMI(Geographical Miss Index) Tol: 0 = no miss, 1 = entire reference volumes have been missed by evaluation contour.

breathing patterns. The primary focus was on replicating a typical clinical pathway, utilizing actual irregular breathing patterns observed in the clinic for tasks such as target delineation, dose prescription, and treatment optimization. It is important to note that caution should be exercised, as there is a potential for underestimating or overestimating the range of motion of the patient's tumor. To address this, various authors have recommended the creation of customized planning target volume (PTV) margins [3,7].

To evaluated the positional and volume inaccuracies in 4D-CT resulting from irregular breathing. According to the commercial 4DCT procedures can both overestimate and underestimate tumor breathing motion. The assessed the robustness of the mid ventilation technique in the presence of variable breathing patterns. Introduced a novel 5DCT technique that combines a recorded surrogate signal with multiple high-pitch 3DCT scans and deformable image registration maps parameterized by breathing amplitude and rate. To investigated 3DCT and 4DCT for irregular breathing traces to enhance tumor movements, average tumor densities, and facilitate the delivery of volumetric modulated arc therapy (VMAT) programs with respectable dosimetric precision.

The assessed the precision of using the external breathing signal to directly rebuild peak-phase and mid-ventilation four-dimensional (4D) computed tomography (CT) frames. Came to the conclusion that 4DCT shows mean tumor motion rather than maximum tumor amplitude when there is irregular breathing. On the other hand, our outlining technique yielded a number for tumor motion that was within 2 mm of the expected amplitude for the regular sine wave "control" trace. There is a fundamental difference in the relationship between the appearance of artefact and breathing trace irregularity in 4D-CBCT image slices compared to 4DCT image slices, which are acquired consecutively. Therefore, using this method ensures that the tumor receives a therapeutic dose during therapy administration and offers an independent confirmation of the accuracy of the pre-treatment imaging. 4DCT-A pictures of the type reported [7] show no image gaps, despite the high degree of irregularity in the breathing traces. This could be explained by two things: To ensure proper coverage of the breathing traces, an online evaluation of the bin distribution was done for each scan. A different CT scanner and reconstruction technique than those utilized by those authors could be the second issue.

Few researchers have conducted comparable

dosimetric analyses for irregular breathers, which makes it difficult to interpret these results. In a retrospective investigation of twenty-three individuals with lung cancer, replicated irregular breathing motion within a TPS. The authors arrived at the conclusion that the dosimetric effects on target coverage (Dmin) were minor at 2.5% for "characteristic" irregular motion, which is the reproduction of irregularities during 4DCT at treatment. These findings are therefore broadly similar with our findings. In the event of "uncharacteristic" anomalies, that is, a systematic change in CTV mobility between imaging and treatment, they do, however, also recommend care. In this instance, a far greater decline in CTV coverage—roughly 10%—was documented.

The findings provide valuable insights into radiotherapy planning and delivery in cases where breathing irregularities are common. The study's results emphasize the importance of 4DCT imaging in these scenarios, particularly for assessing mean tumor motion in the presence of irregular breathing. The research also emphasizes the significance of obtaining accurate and reliable pre-treatment images and ensuring that the therapeutic dose reaches the tumor during treatment delivery, despite the challenges posed by irregular breathing. While some prior studies have explored the dosimetric effects of irregular motion on target coverage, this research contributes to our understanding of the topic. It highlights the need for caution when dealing with uncharacteristic irregularities in breathing patterns, where systematic shifts in target motion can significantly impact coverage.

A comparable phantom investigation was conducted by Santhanam et al. (2009), who reported an acceptable mean discrepancy of 2% in the high-dose zone of a programmable moving phantom and elsewhere. At last, in the context of lung SBRT, Pan et al. (2019) examined the impact of erratic breathing on target doses within a moving phantom. In order to prepare a commercial 4D CBCT system for clinical use, examined the effects of breathing patterns and scanning parameters, sometimes referred to as the scanning sequence, on the image quality and estimated tumor trajectory accuracy. The Quasar phantom was utilized to evaluate the image quality of the 4D CBCT throughout every respiratory phase, with the lung tumor target.

In order to evaluate lung tumor mobility, to create a novel technique based on Dynamic Chest Radiography (DCR) and free analysis software. DCR is a potential modality for lung tumor motion monitoring during radiation, offering various advantages over other approaches, especially fluoroscopy utilizing an X-ray simulator. In order to evaluate deviceless and conventional 4D CT for lung tumor radiation therapy, used a multicell 4D phantom that mimics the movement of the patient during breathing with respect to the target volume, target location, and internal target volume.

The investigation employed two different commercial 4DCT protocols with varying pitch values to evaluate the impact of changes in scanning parameters. Recognizing errors in tumor motion measurement as systematic, akin to clinical 4DCT sessions providing a singular tumor motion displacement value per patient, the study identified over- and under-determined motion amplitudes by averaging the highest and lowest 5% of recorded motions, respectively. As outlined, this process was iterated for tumor sizes ranging from 1 to 4 cm in 1 cm increments, along with tumor motions ranging from 1 to 4 cm in 1 cm increments.

Nevertheless, the study is not exempt from limitations. The utilization of a unidirectional, rigid phantom falls short of fully replicating the clinical scenario, where tumor motion can be deformable and multidirectional. Additionally, the findings are context-specific to the particular scanner, protocol, and treatment platform employed, introducing variability that may exist across diverse clinical settings.

In conclusion, this paper presents a phantom study aimed at assessing the effectiveness of tumor-restricted s4DCT in mitigating phase errors, yielding valuable insights and promising outcomes. The research addresses a crucial concern in radiation therapy: the precision of tumor localization amidst irregular and variable breathing patterns, a common challenge in clinical practice with significant implications for treatment outcomes. The study's results provide compelling evidence that tumor-restricted s4DCT offers a practical solution to reduce phase errors. By confining the scan to the region of interest (ROI) around the tumor, employing a finer slice thickness of 1.25mm, and optimizing scanning times, this approach demonstrates its potential to markedly improve the accuracy of tumor delineation and, consequently, treatment planning.

The study's rigorous methodology, incorporating variations in breathing periods and longitudinal tumor shifts, enhances the credibility of the findings by simulating real-world scenarios. The systematic presentation of comparisons between diverse scan parameters, exposure times, and image volumes underscores the advantages of employing tumor-restricted s4DCT. Beyond its technical contributions to radiation therapy, this research holds promise for elevating the quality of patient care. The reduction of phase errors ensures precise delivery of radiation doses to the tumor while minimizing harm to healthy surrounding tissue. Such improvements can translate into better treatment outcomes, diminished side effects, and heightened patient safety.

Author Contribution Statement

Concept and data collection by Arun Balakrishnan, Guidance and supervision by P. Ramesh Babu; Manuscript evaluation and modification by Arun Balakrishnan and P. Ramesh Babu.

Acknowledgements

Arun Balakrishnan is grateful for the support from Clinician colleagues, Senior Consultants Dr. Rimpa Achari, Dr. Sanjoy Chatterjee, Dr. Indranil Mallick, Dr. Santam Chakraborty, Dr. Moses ArunSingh, Dr. Tapesh Bhattacharjee and My Physics colleagues.

Approval

If it was approved by any scientific Body/ if it is part of an approved student thesis- Yes, Approved by Institution Review Board, Protocol Waiver NO: EC/WV/TMC/01/24.

Ethical Declaration

How the ethical issue was handled (name the ethical committee that approved the research)- This project involves publicly available datasets. This study is not involved with any patients or any healthy volunteers. Approved by Institution Review Board, Protocol Waiver NO: EC/WV/TMC/01/24.

Data Availability

(If apply to your research) Data is available on request.

Conflict of Interest

Authors declare no conflict of Interest.

References

1. Keall PJ, Vedam SS, George R, Williamson JF. Respiratory regularity gated 4d ct acquisition: Concepts and proof of principle. Australas Phys Eng Sci Med. 2007;30(3):211-20. https://doi.org/10.1007/bf03178428.
2. Andronikou S, Chopra M, Langton-Hewer S, Maier P, Green J, Norbury E, et al. Technique, pitfalls, quality, radiation dose and findings of dynamic 4-dimensional computed tomography for airway imaging in infants and children. Pediatr Radiol. 2019;49(5):678-86. https://doi.org/10.1007/s00247-018-04338-5.
3. Aznar MC, Persson GF, Kofoed IM, Nygaard DE, Korreman SS. Irregular breathing during 4dct scanning of lung cancer patients: Is the midventilation approach robust? Phys Med. 2014;30(1):69-75. https://doi.org/10.1016/j.ejmp.2013.03.003.
4. Caines R, Sisson NK, Rowbottom CG. 4dct and vmat for lung patients with irregular breathing. J Appl Clin Med Phys. 2022;23(1):e13453. https://doi.org/10.1002/acm2.13453.
5. Chen Y, Gong G, Wang Y, Liu C, Su Y, Wang L, et al. Comparative evaluation of 4-dimensional computed tomography and 4-dimensional magnetic resonance imaging to delineate the target of primary liver cancer. Technol Cancer Res Treat. 2021;20:15330338211045499. https://doi.org/10.1177/15330338211045499.
6. Wulfhekel E, Grohmann C, Gauer T, Werner R. Ep-1743: Compilation of a database for illustration and automated detection of 4dct motion artifacts. Radiotherapy and Oncology. 2014;111:S266. https://doi.org/10.1016/S0167-8140(15)31861-2.
7. Matsumura N, Oki S, Fukasawa N, Matsumoto M, Nakamura M, Nagura T, et al. Glenohumeral translation during active external rotation with the shoulder abducted in cases with glenohumeral instability: A 4-dimensional computed tomography analysis. J Shoulder Elbow Surg. 2019;28(10):1903-10. https://doi.org/10.1016/j.jse.2019.03.008.
8. Doi Y, Shimohigashi Y, Kai Y, Maruyama M, Toya R. Validation of four-dimensional computed tomography without external reference respiratory signals for radiation treatment planning of lung tumors. Biomed Phys Eng Express. 2022;8(5). https://doi.org/10.1088/2057-1976/ac8555.
9. Dou TH, Thomas DH, O'Connell D, Bradley JD, Lamb JM, Low DA. Technical note: Simulation of 4dct tumor motion measurement errors. Med Phys. 2015;42(10):6084-9. https://doi.org/10.1118/1.4931416.
10. Choi J-H, Lee S. Real-time tumor motion tracking in 3d using planning 4d ct images during image-guided radiation therapy. Algorithms. 2018;11:155. https://doi.org/10.3390/a11100155.
11. Eller M, Dave A, Johnson C, Fingeret AL. Accuracy of 4-dimensional computed tomography for localization in primary hyperparathyroidism. J Surg Res. 2021;257:15-21. https://doi.org/10.1016/j.jss.2020.07.055.
12. Ko YE, Song SY, Je HU. Practical usefulness of partial-range 4-dimensional computed tomography in the simulation process of lung stereotactic body radiation therapy. Radiation Physics and Chemistry. 2022;201:110437. https://doi.org/https://doi.org/10.1016/j.radphyschem.2022.110437.
13. Pattanayak L, Mohanta S, Panda S, Mohapatra M. Comparison of dosimetric data of bone marrow between standard imrt and bone marrow sparing imrt in carcinoma cervix. Rep Pract Oncol Radiother. 2021;26(6):976-83. https://doi.org/10.5603/RPOR.a2021.0120.
14. Guckenberger M, Wilbert J, Krieger T, Richter A, Baier K, Flentje M. Mid-ventilation concept for mobile pulmonary tumors: Internal tumor trajectory versus selective reconstruction of four-dimensional computed tomography frames based on external breathing motion. Int J Radiat Oncol Biol Phys. 2009;74(2):602-9. https://doi.org/10.1016/j.ijrobp.2008.12.062.
15. Juhler Nøttrup T, Korreman SS, Pedersen AN, Aarup LR, Nyström H, Olsen M, et al. Intra- and interfraction breathing variations during curative radiotherapy for lung cancer. Radiother Oncol. 2007;84(1):40-8. https://doi.org/10.1016/j.radonc.2007.05.026.
16. Abdelnour AF, Nehmeh SA, Pan T, Humm JL, Vernon P, Schöder H, et al. Phase and amplitude binning for 4d-ct imaging. Phys Med Biol. 2007;52(12):3515-29. https://doi.org/10.1088/0031-9155/52/12/012.
17. Kitamura K, Takayama K, Yamazaki R, Ueda Y, Nishiki S. A new method for assessing lung tumor motion in radiotherapy using dynamic chest radiography. J Appl Clin Med Phys. 2022;23(10):e13736. https://doi.org/10.1002/acm2.13736.
18. George R, Vedam SS, Chung TD, Ramakrishnan V, Keall PJ. The application of the sinusoidal model to lung cancer patient respiratory motion. Med Phys. 2005;32(9):2850-61. https://doi.org/10.1118/1.2001220.
19. Lee S, Yan G, Lu B, Kahler D, Li JG, Sanjiv SS. Impact of scanning parameters and breathing patterns on image quality and accuracy of tumor motion reconstruction in 4d cbct: A phantom study. J Appl Clin Med Phys. 2015;16(6):195-212. https://doi.org/10.1120/jacmp.v16i6.5620.
20. Liu H, Kholinne E, Sun Y, Liu T, Tan J. The dynamic rotation axis of ulnohumeral joint during active flexion-extension: An in vivo 4-dimensional computed tomography analysis. BMC Musculoskelet Disord. 2022;23(1):152. https://doi.org/10.1186/s12891-022-05102-5.
21. Low DA, Parikh PJ, Lu W, Dempsey JF, Wahab SH, Hubenschmidt JP, et al. Novel breathing motion model for radiotherapy. Int J Radiat Oncol Biol Phys. 2005;63(3):921-9. https://doi.org/10.1016/j.ijrobp.2005.03.070.
22. Morris M, Eifel PJ, Lu J, Grigsby PW, Levenback C, Stevens RE, et al. Pelvic radiation with concurrent chemotherapy compared with pelvic and para-aortic radiation for high-risk cervical cancer. N Engl J Med. 1999;340(15):1137-43. https://doi.org/10.1056/nejm199904153401501.
23. Manohar A, Colvert GM, Yang J, Chen Z, Ledesma-Carbayo MJ, Kronborg MB, et al. Prediction of cardiac resynchronization therapy response using a lead placement score derived from 4-dimensional computed tomography.

Circ Cardiovasc Imaging. 2022;15(8):e014165. https://doi.org/10.1161/circimaging.122.014165.
24. Mafi M, Moghadam SM. Real-time prediction of tumor motion using a dynamic neural network. Med Biol Eng Comput. 2020;58(3):529-39. https://doi.org/10.1007/s11517-019-02096-6.
25. Miller R, Castillo R, Castillo E, Jones BL, Miften M, Kavanagh B, et al. Characterizing pulmonary function test changes for patients with lung cancer treated on a 2-institution, 4-dimensional computed tomography-ventilation functional avoidance prospective clinical trial. Adv Radiat Oncol. 2023;8(2):101133. https://doi.org/10.1016/j.adro.2022.101133.
26. Morton N, O'Brien R, Keall P, Reynolds T. System requirements to improve adaptive 4-dimensional computed tomography (4d ct) imaging. Biomed Phys Eng Express. 2022;8(6). https://doi.org/10.1088/2057-1976/ac9849.
27. Mutaf YD, Scicutella CJ, Michalski D, Fallon K, Brandner ED, Bednarz G, et al. A simulation study of irregular respiratory motion and its dosimetric impact on lung tumors. Phys Med Biol. 2011;56(3):845-59. https://doi.org/10.1088/0031-9155/56/3/019.
28. Peng J, Gong J, Wang X, Mou J, Xu H, Dai J, et al. 4-dimensional computed tomography analysis of clinical target volume displacement in adjuvant radiation of patients with gastric cancer and its implication on radiotherapy. Oncol Lett. 2019;17(4):3641-8. https://doi.org/10.3892/ol.2019.10037.
29. Richter A, Wilbert J, Flentje M. Dosimetric evaluation of intrafractional tumor motion by means of a robot driven phantom. Med Phys. 2011;38(10):5280-9. https://doi.org/10.1118/1.3633890.
30. Santhanam A, Willoughby TR, Meeks SL, Rolland JP, Kupelian PA. Modeling simulation and visualization of conformal 3d lung tumor dosimetry. Phys Med Biol. 2009;54(20):6165-80. https://doi.org/10.1088/0031-9155/54/20/009.
31. Sarker J, Chu A, Mui K, Wolfgang JA, Hirsch AE, Chen GT, et al. Variations in tumor size and position due to irregular breathing in 4d-ct: A simulation study. Med Phys. 2010;37(3):1254-60. https://doi.org/10.1118/1.3298007.
32. Shakoor D, Hafezi-Nejad N, Haj-Mirzaian A, Shores JT, Lifchez SD, Morelli JN, et al. Kinematic analysis of the distal radioulnar joint in asymptomatic wrists using 4-dimensional computed tomography-motion pattern and interreader reliability. J Comput Assist Tomogr. 2019;43(3):392-8. https://doi.org/10.1097/rct.0000000000000839.
33. Grootjans W, Dhont J, Gobets B, Verellen D. Management of respiratory-induced tumour motion for tailoring target volumes during radiation therapy. 2020. p. 47-68.
34. Sharifi H, Brown S, McDonald GC, Chetty IJ, Zhong H. 4-dimensional computed tomography-based ventilation and compliance images for quantification of radiation-induced changes in pulmonary function. J Med Imaging Radiat Oncol. 2019;63(3):370-7. https://doi.org/10.1111/1754-9485.12881.
35. Sisson nk, caines r, egleston d, rowbottom cg. Should 4dct be used for radiotherapy patients with irregular breathing. Rad mag. 2019 mar; 45:19-20.
36. Thomas D, Lamb J, White B, Jani S, Gaudio S, Lee P, et al. A novel fast helical 4d-ct acquisition technique to generate low-noise sorting artifact-free images at user-selected breathing phases. Int J Radiat Oncol Biol Phys. 2014;89(1):191-8. https://doi.org/10.1016/j.ijrobp.2014.01.016.
37. Ueda Y, Tsujii M, Ohira S, Sumida I, Miyazaki M, Teshima T. Residual set up errors of the surrogate-guided registration using four-dimensional ct images and breath holding ones in respiratory gated radiotherapy for liver cancer. In Vivo. 2021;35(4):2089-98. https://doi.org/10.21873/invivo.12478.
38. Umezawa R, Wakita A, Katsuta Y, Ito Y, Nakamura S, Okamoto H, et al. A pilot study of synchronization of respiration-induced motions in the duodenum and stomach for the primary tumor in radiation therapy for pancreatic cancer using 4-dimensional computed tomography. Adv Radiat Oncol. 2021;6(4):100730. https://doi.org/10.1016/j.adro.2021.100730.
39. Wu J, Liu J, Wang J, Li J, Gu S, Yao Y, et al. Imaging features of cardioembolic stroke on 4-dimensional computed tomography angiography. Quant Imaging Med Surg. 2023;13(9):6026-36. https://doi.org/10.21037/qims-23-120.
40. Chi A, Nguyen NP. 4d pet/ct as a strategy to reduce respiratory motion artifacts in fdg-pet/ct. Front Oncol. 2014;4:205. https://doi.org/10.3389/fonc.2014.00205.
41. Yang W, Hong JY, Kim JY, Paik SH, Lee SH, Park JS, et al. A novel singular value decomposition-based denoising method in 4-dimensional computed tomography of the brain in stroke patients with statistical evaluation. Sensors (Basel). 2020;20(11). https://doi.org/10.3390/s20113063.